Effect of molecular weight on rolled high density polyethylene: 1. Structure, morphology and anisotropic mechanical behaviour

Min-Diaw Wang, Eiji Nakanishi* and Sadao Hibi
Department of Materials Science and Engineering, Nagoya Institute of Technology, Gokiso-cho, Showa-ku, Nagoya 466, Japan
(Received 4 June 1992; revised 4 September 1992)

Rolled high density polyethylene with various molecular weights was used to study the effect of primary structure on the properties of the material. Keeping the molecular weight distribution at 2, and with similar processing conditions, it was found that the structure, morphology and anisotropic mechanical behaviour depended strongly on the molecular weight. The low molecular weight samples possessed high modulus and yield stress in the roll direction and showed brittle fracture in the direction perpendicular to the roll direction. The high molecular weight samples showed high modulus and yield stress in the direction perpendicular to the roll direction. The morphology of the internal surface showed a transitional change from fibrillar structure for low molecular weight samples to a smooth surface for high molecular weight samples. Wide angle X-ray diffraction revealed that, for samples with high molecular weight, the crystallographic axes were selectively correlated with the coordinate axes used in defining the samples. Small angle X-ray scattering showed four-point patterns for high molecular weight samples. It is suggested that samples with high molecular weight possess more entanglements among the tie chains connecting the lamella blocks. This results in higher orientation of the three crystallographic axes, *a*, *b* and *c*, along the thickness, transverse and roll directions of the sample, respectively. Entanglement also reduces the anisotropic behaviour in the roll–transverse plane.

(Keywords: high density polyethylene; molecular weight; rolled; orientation; morphology; anisotropic behaviour)

INTRODUCTION

Anisotropy has been an important subject for polymer science ever since the practical application of polymeric materials. Keller[1–8], Rider[9–11], Meinel and Peterlin[12–15] and Kawai[16,17] and their co-workers have studied the deformation mechanism of crystalline polymers. They have reported the breakdown of spherulites into a lamellar structure during deformation. Chain slippage along the (1 0 0) plane resulted in inclination of the normal of the lamella plane from the draw or roll direction (machine direction, MD) which is consistent with the chain axis. For polyethylene (PE), heat treatment would result in rotation of the lamella block around the *b*-axis while the inclination between the normal of the lamella plane and the chain axis would not be changed. Poly(ethylene terephthalate) (PET) has been extensively studied by Brown, Ward and co-workers[18–25], who reported the reorientation of the molecular chain inside the slip band and kink band during off-angle redrawing. In both cases, the polymer chain was reoriented towards the redraw direction. The angle between the band direction and the MD is quite different for slip band and for kink band. This stimulated study of the formation of the kink band in polymers. Superficially the kink deformation of polymeric materials is quite similar to that of metals. However, the intrinsic difference between these two materials certainly implies different deformation mechanisms and research has proved this, although common agreement has not been reached[26–29]. Hibi *et al.*[30] simulated the orientation distribution of chain axes of various polymers by assuming affine deformation of the lamellae. For rolled PE, the *c*-axis is oriented in the roll direction (MD) while the *a*-axis is oriented in the thickness direction (the direction parallel to the normal of the film, ND). They suggested that the *a*-axis always orients in the direction perpendicular to the maximum shear stress. This has been proved by Katagiri *et al.*[31] who applied combined stress on cylindrically shaped PE and studied the orientation of the crystallographic axes. For most of these studies, effects of processing rather than of the primary structures (e.g. repeat unit, branching, molecular weight and its distribution) have been examined. For PE, the repeat unit is $-CH_2-CH_2-$ and the main chain shows a zigzag structure. Molecular weight seems to be the best candidate for improving physical properties. That is why ultrahigh molecular weight polyethylene (UHMWPE) has been widely used in practical applications. However, the effect of primary structure on anisotropic behaviour has received little attention.

* To whom correspondence should be addressed

0032-3861/93/132783-09

In this paper, high density polyethylene (HDPE), with five different molecular weights but similar molecular weight distributions, was used to study the effect of molecular weight on the structure, morphology and mechanical behaviour under similar processing conditions. These materials were specially designed so that the only difference would be the molecular weight. Wide angle X-ray diffraction (WAXD) was used to study the orientation of the crystallographic axes, while small angle X-ray scattering (SAXS) was used to reveal the textural structure. Scanning electron microscopy (SEM) was applied to study the morphology. The results are correlated with the mechanical behaviour by tensile testing and the effect of molecular weight is discussed. A study of the effect on the fracture behaviour is included in the accompanying paper[32].

EXPERIMENTAL

Five samples of HDPE with different molecular weights were kindly supplied by Toso Ltd. The molecular weight distribution was about 2 for all samples, so that molecular weight was the only variable. The weight average molecular weights (M_w) were 7.4×10^4, 17×10^4, 42×10^4, 61×10^4 and 98×10^4 for samples 1–5, respectively. All the samples were pressed at 200°C and 200 kg cm^{-2} and quenched in cool water. The as-pressed samples were 3 mm thick and were rolled at 115 and 125°C, depending on the processability of the samples. The surface speed of the roller was 23.6 mm min^{-1}. The clearance between the rollers was set as 0.3 mm. Since the recovery of thickness after rolling could not be avoided, the as-rolled ratios were less than 10. Refractive indices in the roll direction (MD), transverse direction (TD) and thickness direction (ND) were measured using an Abbe refractometer. Density was measured using a density column at 24°C. The basic data of the samples are summarized in *Table 1*. Sample 1 possessed the lowest M_w and high birefringence compared to other samples. In order to obtain similar molecular orientation (similar birefringence) to sample 1, samples 2 and 3 were further stretched at the roll temperature; the stretch speeds were higher than the roller speed and were set to obtain the required birefringence, so were different for samples 2 and 3. Stretching was performed immediately when materials came out of the rollers, so that rolling and stretching should be considered as one process. Samples of this kind are denoted as 2b and 3b, to distinguish them from samples 2a and 3a which were processed using the same conditions as samples 1, 4 and 5. Samples 4 and 5 could not be drawn further due to the strong retraction.

WAXD was carried out using a Jeol X-ray generator at 36 kV and 13 mA. Diffraction patterns were taken by shooting the X-ray through the thickness direction (through view, ND) and through the width direction (edge view, TD). SAXS was observed using a Rigaku X-ray generator at 40 kV and 20 mA. In addition to the ND and TD directions, SAXS patterns were also taken by shooting the X-ray through the roll direction (end view, MD), although for most cases distinct diffraction patterns were not obtained.

The morphology of the rolled sample was studied using a scanning electron microscope (Jeol JSM-820). Surface pictures of the internal layer of each sample were taken. To study the anisotropic mechanical behaviour, rectangular pieces making various off-angles to the roll direction were cut from each sample. The test specimen was 60 mm between the gauges and 20 mm in width. The stretch speed was 5% min^{-1}. The Young's modulus was taken by dividing the stress by the strain at a strain of 0.5%. The yield stress was defined as the intersect of the initial slope and the tangential line from strain at 3%.

Table 1 Basic properties of the samples

Group	No.	M_w (10^4)	Δ^a	$\sum n/3$	$T_{proc.}$ (°C)
I	2a	17	0.0472	1.5442	115
	3a	42	0.0418	1.5411	115
	4	61	0.0396	1.5421	125
	5	98	0.0410	1.5431	125
II	1	7.4	0.0499	1.5462	115
	2b	17	0.0510	1.5440	115
	3b	42	0.0496	1.5440	115

[a] Birefringence, $n_{MD} - n_{TD}$

RESULTS AND DISCUSSION

The materials were divided into two groups depending on the extent of chain orientation. Group I included samples 2a, 3a, 4 and 5. These samples were rolled without further drawing. Group II included samples 1, 2b and 3b. Sample 1 was not stretched further during rolling but its birefringence was quite close to that of samples 2b and 3b which were stretched. Each group contained samples with various molecular weights. There were also samples of the same molecular weight (samples 2 and 3) in each group.

Figure 1 shows the density of the pressed and deformed samples. The smaller the molecular weight, the higher the density became. Rolling resulted in a increase in density due to the high processing temperature. The density of rolled samples 4 and 5 was higher than that of sample 3a because the processing temperatures were different. Basically, the relationship between the density and the molecular weight of the rolled samples was the same as that of the original samples. The density of sample

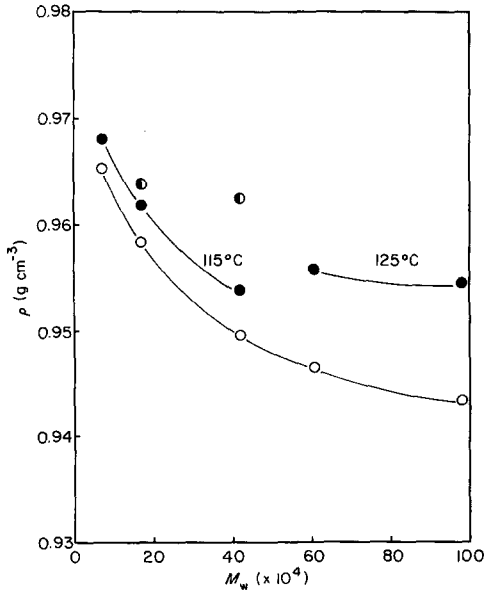

Figure 1 Dependence of density on molecular weight: ○, samples pressed at 200°C; ●, samples rolled at temperature indicated; ◐, samples further stretched after rolling at 115°C

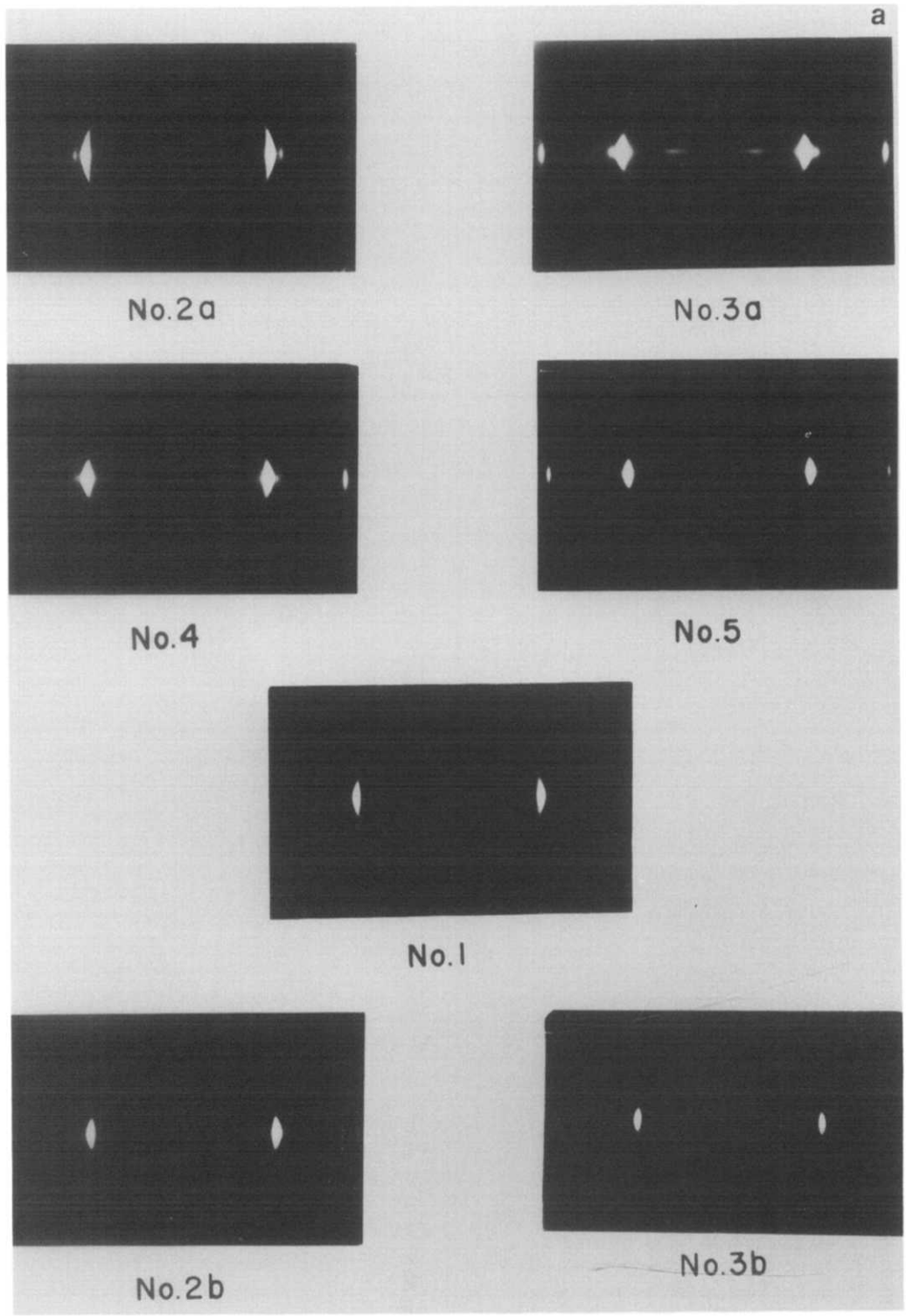

Figure 2 WAXD patterns of the samples: (a) through view (patterns taken from the ND); (b) edge view (patterns taken from the TD). MD is in the vertical direction

2b was quite close to that of 2a while samples 3b and 3a were quite different in density. This difference will be discussed after further results are presented. *Figure 2* shows WAXD patterns of the specimens. For PE, the (1 1 0), (0 2 0) and (2 0 0) planes are convenient in interpreting the orientation of the crystallographic axes. The ND patterns (*Figure 2a*) showed spots of the (0 2 0) plane diffraction in the equatorial direction, which implied orientation of the *b*-axis in the TD. As the molecular weight became smaller, the spot patterns spread slightly into arcs for group II samples. Strong diffraction of the (2 0 0) plane can be observed in *Figure 2b* while diffraction of the (0 2 0) plane disappeared completely. Basically, the *c*-axis aligned in the MD, the *b*-axis in the TD and the *a*-axis in the ND. From *Figure 2*, this pattern of orientation was strong for high molecular weight samples and became weaker for the low molecular weight samples. Comparison of group I and II shows that further stretching resulted in stronger orientation.

The textural structure can be realized from the SAXS pattern. In *Figure 3a*, the ND diffraction pattern shows two-point patterns for all the group II samples and for sample 2a in group I. For group II, the higher the

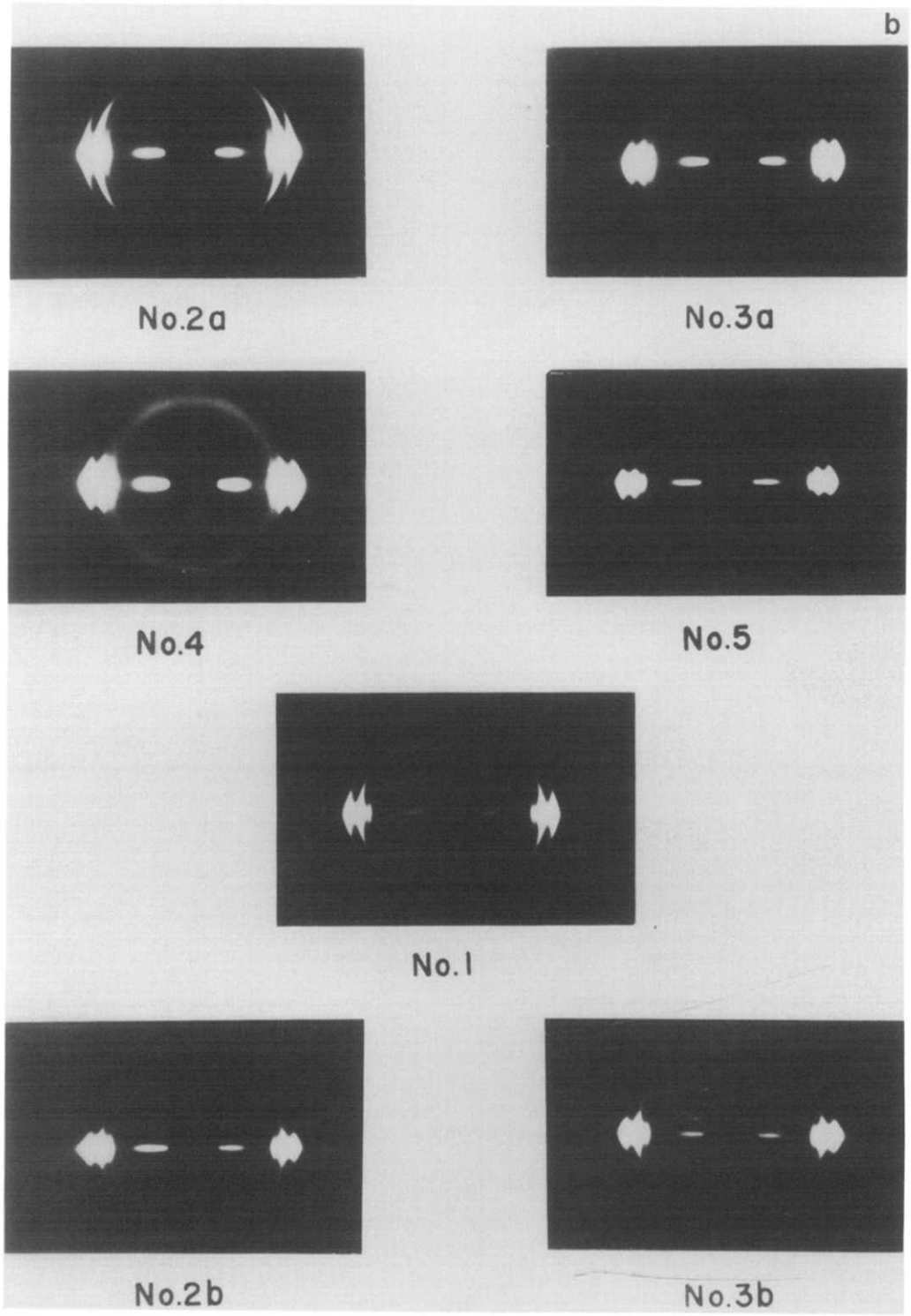

Figure 2 *(continued)*

molecular weight, the larger was the long period spacing. Because the patterns of samples 3a, 4 and 5 were not well defined, direct comparison of the long period spacing of the group I samples was not possible at this point. But it seems that samples with higher molecular weight also possessed greater long period spacing. Four-point patterns, which imply inclination of the normal of the lamella from the MD, are shown in *Figure 3b*. For group I samples, both the angle of inclination (ϕ) and the long period spacing became larger as the molecular weight increased. The idealized model of the textural structure is shown in *Figure 3d*. The inclination of the lamella plane was similar to that observed by Keller[1–4] and was interpreted as due to slippage of the (1 0 0) plane. Heat treatment of the rolled PE showed rotation of the lamella blocks around the *b*-axis, which depended mainly on the chains connecting the lamella blocks[2]. Group II samples showed patterns with smaller ϕ. The diffraction patterns with the X-ray along the MD were not well defined and only the pattern of sample 3a is shown in *Figure 3c* as a typical example. The ill-defined pattern was due to the large value of ϕ of the normal of the lamella plane from the MD. The value of ϕ and the long period spacing are summarized in *Table 2*. The long period spacing is

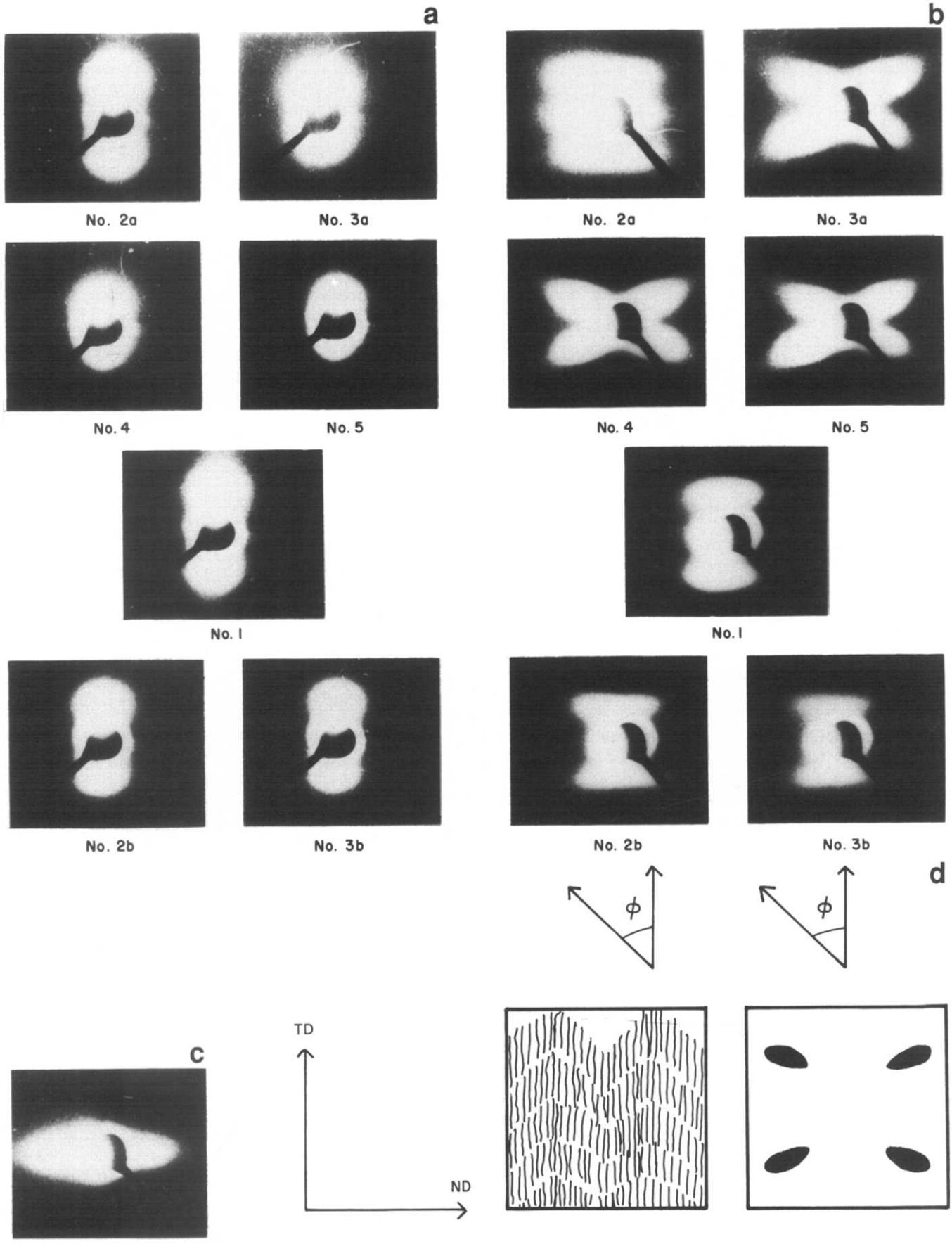

Figure 3 SAXS patterns of the samples: (a) through view; (b) edge view; (c) end view of sample 3a (pattern taken from the MD); (d) ideal model of the texture corresponding to the edge view pattern. The vertical direction is the MD for (a), (b) and (d) and the TD for (c)

Table 2 Long period spacing and angle of inclination (ϕ) from SAXS

Group	No.	d_{ND} (Å)	d_{TD} (Å)	ϕ_{TD}	d_{0TD} (Å)[a]
I	2a	132.62	116.04	33(arc)	138.36
	3a	–	99.47	55	173.42
	4	–	111.40	59	216.29
	5	–	126.59	62	269.64
II	1	126.60	111.40	20(arc)	111.41
	2b	135.85	111.12	35	135.65
	3b	142.82	116.04	40.5	152.60

[a] From equation (1)

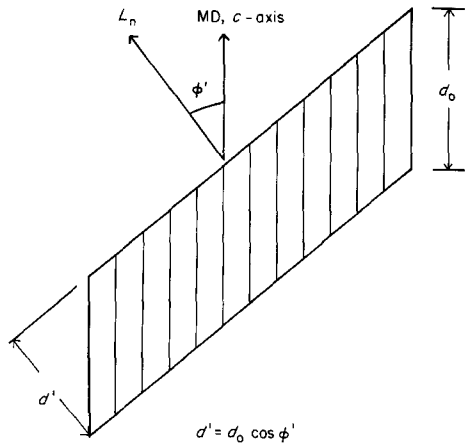

Figure 4 Ideal model showing the relation between ϕ and ϕ'

composed of the lamella thickness and the amorphous region between lamella blocks. As the crystallinity is high, it is reasonable to take the crystalline and amorphous regions as a block during deformation. Consider the idealized model shown in *Figure 4*, which shows the block of highly crystalline PE as mentioned above. This is viewed through the TD. Let the long period spacing of the lamella be defined as d_0 and the angle of inclination between the lamella normal and the chain axis (MD) as ϕ'. Then the long period spacing measured from the TD SAXS diffraction pattern, d', can be expressed as:

$$d' = d_0 \cos \phi' \quad (1)$$

If the angle of inclination is changed from ϕ' to ϕ'' due to more chain slippage, the new long period spacing should be:

$$d'' = d'(\cos \phi''/\cos \phi') \quad (2)$$

That is to say, if further stretching immediately after rolling (at the same temperature) results in further chain slippage along the (1 0 0) plane only, the long period spacing of a sample which is stretched further can be evaluated from that of the rolled sample according to equation (2). The calculated value was 113.3 Å for sample 2b and 131.8 Å for sample 3b using the data from samples 2a and 3a in *Table 2*. For sample 2b, the calculated result was quite consistent with the measurement, while sample 3b showed a difference as large as 15 Å between the calculation and the measurement. Also, further stretching after rolling of sample 3 decreased ϕ from 55° to 40°. This, together with the large increase in density (*Figure 1*), indicates that the mechanism of deformation from sample 3a to 3b was quite different from that for samples 2a and 2b. A possible explanation is that further stretching and rolling resulted in smaller lamella blocks and recrystallization under stress occurred due to the high processing temperature for sample 3b. A certain extent of stress relaxation due to breakdown of lamella blocks should occur during the deformation, so that ϕ would become smaller. From equation (1) and the long period spacing from TD, it was found that the d_0 value increased with increase of molecular weight, which implied larger lamella blocks or increased spacing among the lamella blocks, or both. The larger the lamella block, the larger ϕ became. This is one reason why processing of high molecular weight samples required a much higher torque, which was consumed during the chain slippage. The greater orientation of the crystallographic axes relative to the sample axes for high molecular weight samples implies that more entanglements existed among the tie chains connecting the lamella blocks, which helped in arranging the layout of the crystalline texture.

It seems that conflict exists between the birefringence (*Table 1*) and X-ray results. Samples showing an arc pattern rather than a spot diffraction pattern possessed higher birefringence, e.g. samples 1 and 3b. One explanation could be the difference in crystallinity. It is commonly accepted that the birefringence of a semicrystalline polymer can be expressed as follows, assuming two-phase structure:

$$\Delta n = (\Delta n)_{max}[1 - 3/2\langle \sin^2 \theta \rangle]$$
$$(\Delta n)_{max} = V_c(\Delta n^c)_{max} + (1 - V_c)(\Delta n^a)_{max} \quad (3)$$

where V_c is the volume fraction of the crystalline region, $(\Delta n^c)_{max}$ and $(\Delta n^a)_{max}$ represent the intrinsic birefringence of the crystalline and amorphous regions, respectively. $\langle \mathrm{Sin}^2 \theta \rangle$ represents the orientation factor based on the MD; in the case of perfect alignment of the *c*-axis in the MD, this value is zero, but if the *c*-axis lies in the TD–ND plane, it will be one. Higher crystallinity results in higher $(\Delta n^c)_{max}$ which leads to higher birefringence. The difference in crystallinity for samples 1 and 3b was about 4%. This could complement, to some extent, the difference in $\langle \sin^2 \theta \rangle$. However, this explanation is not valid in the case of the sample 2a.

The rolled samples possessed a layered structure. After peeling off the surface layer, it was possible to study the morphology of the materials. *Figure 5* shows the SEM pictures of the samples with the MD in the horizontal direction. The magnification was 2000×. The group I samples showed a smoother structure than the group II samples. Whitened parts, indicating highly plastic deformation due to peeling, were observed especially for samples 4 and 5. Compared with the other samples in group I, sample 2a showed fewer whitened parts and some fibrillar structure appeared. For group II samples, a quite different surface structure was observed. Sample 1 showed a rough fracture surface with little plastic deformation. Sample 2b consisted of bundles of fibre. Sample 3b showed fibrillar structure with plastically deformed parts. The connection between bundles of fibre of sample 3b is believed to be stronger than that of sample 2b. Even the WAXD patterns showed high orientation of the *c*-axis in the MD for samples 4 and 5; the macroscopic structure did not reveal such a pattern.

The anisotropic mechanical behaviour of these samples is shown in *Figures 6* and *7*. *Figure 6* shows the Young's modulus tested at various off-angles in the MD–TD plane. It is interesting to see that high orientation in the roll direction certainly did not result in higher modulus

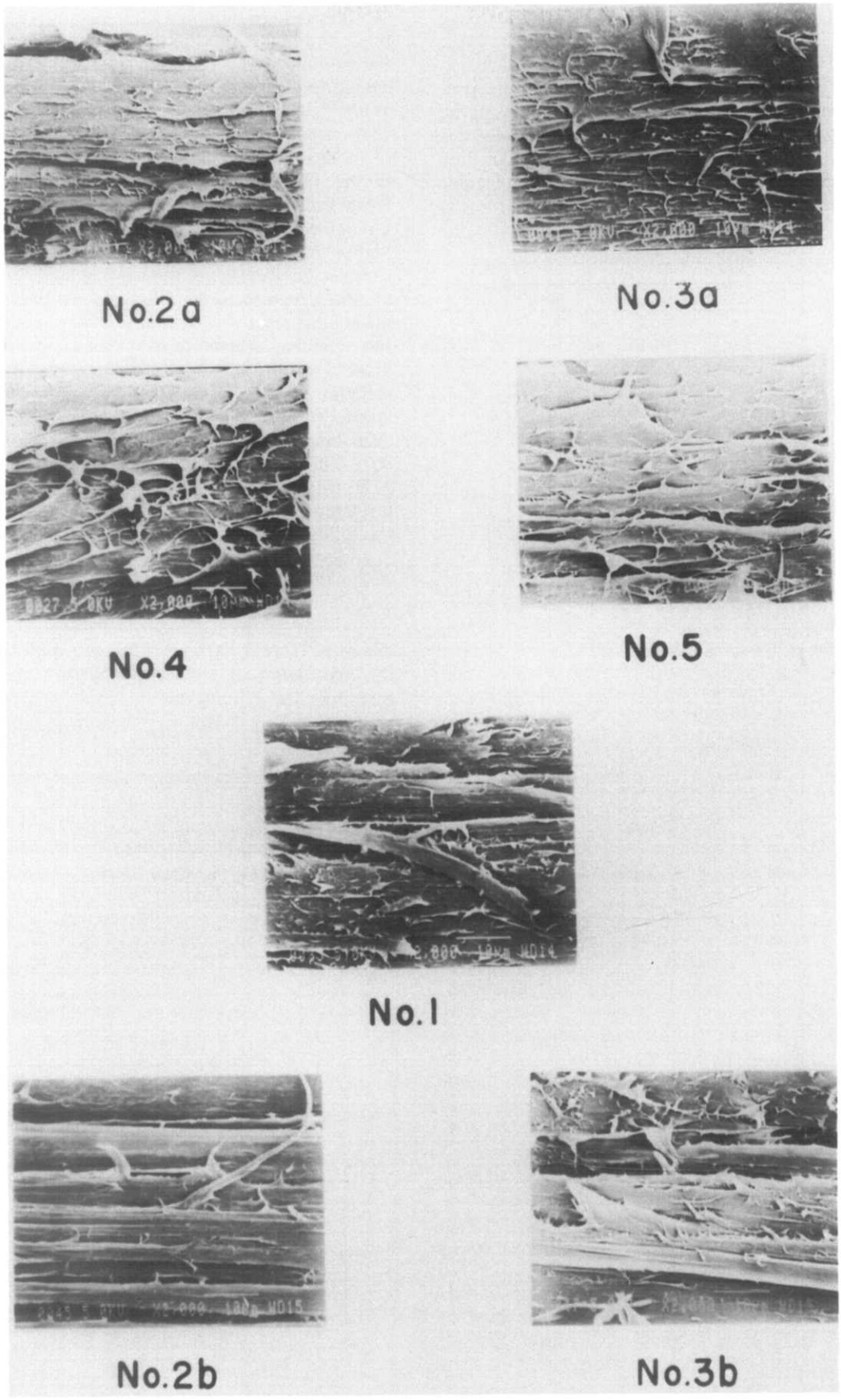

Figure 5 SEM pictures of the internal structure of the samples after peeling off the surface layer. MD is in the horizontal direction

in MD when compared with the modulus in TD (off-angle 90°) for group I samples. According to Tashiro *et al.*[33], the stiffness of the *c*-axis is more than 30 times that of the *a*-axis or *b*-axis. With high crystallinity and high orientation, the samples should show highest modulus in the MD and lowest modulus in the TD, while the experimental data showed otherwise. This could also be related to the effect from the tie chain. For high molecular

weight samples, input energy was relaxed by slippage along the (1 1 0) plane during rolling. As long as the effect of entanglements existed, energy would be dissipated, to some extent, in this way during off-angle testing. Also, disentanglement would help in reducing brittleness in the MD. That is believed to be the reason why high molecular weight samples showed greater toughness than low molecular weight samples. As a result, high molecular weight samples were more ductile in the MD. Group II samples showed quite similar behaviour to each other and possessed higher moduli than group I samples. However, the modulus in the TD was not the minimum. Mechanical evaluation of such phenomena has been discussed by Ward[34]. Although the real mechanism is not clear, it is suggested that rolling in the MD resulted in alignment of the lamella–tie chain structure in the MD. Stretching in the TD would not result in shear deformation, as happened to the other off-angle, except in the MD. This might be the reason why the moduli in the TD were higher than in the other off-angles. Further stretching of samples 2a and 3a resulted in an increase in moduli in all off-angle directions. The yield stress tested at various off-angles is shown in *Figure 7*. In the MD–TD plane, the anisotropic behaviour in yield stress of samples 3a, 4 and 5 was also not so obvious compared with the other samples. For sample 1, the specimens broke in brittle failure at off-angles of 60° and 75° after yielding, and even before yielding when tested in the TD (off-angle 90°). The fracture surface was perfectly parallel to the MD. For isotropic solids, the von Mises yield criterion is referenced most. For anisotropic solids, Hill[35] proposed the following yield criterion:

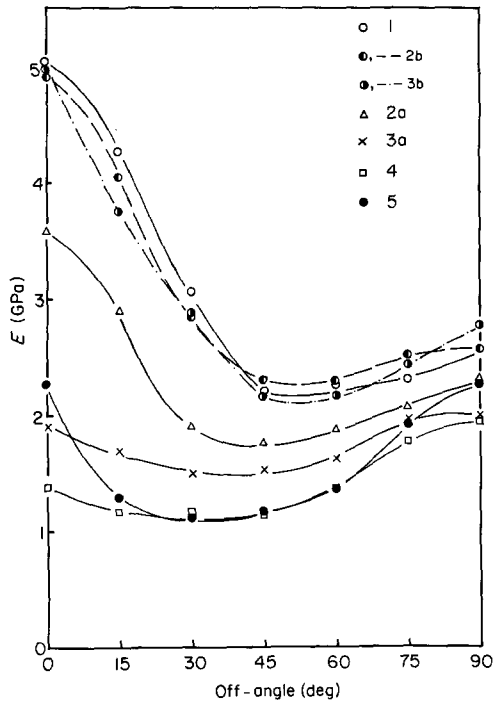

Figure 6 Young's modulus, E, of the samples at various off-angles

$$F(\sigma_y-\sigma_z)^2+G(\sigma_z-\sigma_x)^2+H(\sigma_x-\sigma_y)^2+2L\tau_{xy}^2+2M\tau_{yz}^2+2N\tau_{xy}^2=1 \quad (4)$$

where F, G, H, L, M and N are constants depending on the materials and anisotropy. With z as the thickness direction, let us consider the case of plane stress. The terms including z will vanish and equation (4) can be rewritten as:

$$F\sigma_y^2+G\sigma_x^2+H(\sigma_x-\sigma_y)^2+2L\tau_{xy}^2=1 \quad (5)$$

Furthermore, let us assume the y-axis as the roll direction (MD) and the x-axis as the TD. If the specimen is drawn at $\theta°$ off the MD, the stress in the x and y direction can

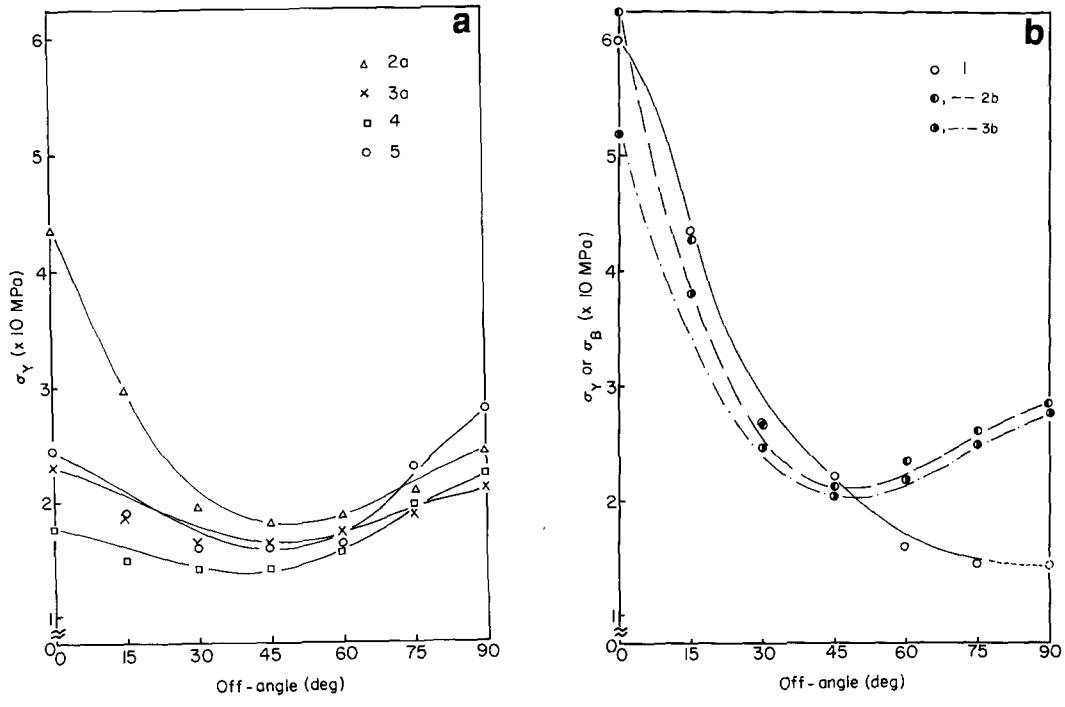

Figure 7 Yield stress and break stress (for sample 1) of the samples at various off-angles: (a) group I; (b) group II. The lines are the results calculated from equation (6) with constants from *Table 3*

Table 3 The anisotropic constants of Hill's theory

Group	No.	$H+G$	$H+F$	$L-H$
I	2a	0.00053	0.00170	0.00502
	3a	0.00189	0.00227	0.00554
	4	0.00327	0.00200	0.00779
	5	0.00167	0.00129	0.00633
II	1	0.00028	0.00474	0.00190
	2b	0.00026	0.00123	0.00339
	3b	0.00037	0.00125	0.00388

be expressed in terms of σ_θ as follows:

$$\sigma_x = \sigma_\theta \cos^2\theta$$
$$\sigma_y = \sigma_\theta \sin^2\theta$$
$$\tau_{xy} = \sigma_\theta \sin\theta\cos\theta \quad (6)$$

and equation (5) can be rewritten as:

$$\sigma_\theta^2\{(H+G)\cos^4\theta + 2(L-H)\sin^2\theta\cos^2\theta + (H+F)\sin^4\theta\} = 1 \quad (7)$$

The constants $(H+G)$, $(H+F)$ and $(L-H)$ can be derived from the yield stress by stretching the anisotropic specimen in the MD, TD and 45° between the MD and TD. When these constants are known, the yield stress in the other off-angle directions can be calculated by equation (7). The calculated $(H+G)$, $(H+F)$ and $(L-H)$ values are listed in *Table 3*. The calculated yield stresses are plotted in *Figure 7* and simulation by Hill's theory was acceptable. Assumption of plane stress can be applied to the materials in this study.

Young's modulus reflects the initial mechanical behaviour while yielding is the start of large deformation. For low molecular weight samples, the chain has been extended to some extent so that, during the test, high anisotropy and high mechanical behaviour were obtained at small deformations. On the other hand, for high molecular weight samples the chains were long and more entanglements existed. Even for the materials that possessed high orientation of the chain axis in the process direction, less anisotropy and low mechanical properties were obtained during the test. This implies that both the anisotropy and the mechanical behaviour should not only be related to the orientation of the chain itself but must also depend on the chains connecting the lamella blocks. As discussed above, slippage along the (1 0 0) plane and disentanglement rather than breakdown of the lamella blocks for high molecular weight samples dissipate the energy input to the system. These should be responsible for the decrease in the moduli and the yield stress. Details of the amorphous region are not clear at present. However, from the above result, its effect cannot be neglected even at crystallinity as high as 70%.

CONCLUSION

With similar processing conditions, fibre structure can be observed for low molecular weight samples only. Further stretching of samples 3a did induce some fibrillar structure while the texture of the lamella blocks was changed. For low molecular weight samples, small lamella blocks are easier to rotate during processing and the energy is consumed in this way rather than by chain slippage inside the lamella structure. For high molecular weight samples, entanglement played an important role in affecting the material structure and properties. With the other primary structure factors kept constant, the only difference was the length of the molecular chain. As a result, the crystallinity was lower, the inclination of the lamellae was larger and the anisotropic mechanical behaviour was not so obvious when compared with the low molecular weight samples. It is believed that the existence of more entanglements among the tie chains connecting the lamella blocks is responsible for the above phenomena.

REFERENCES

1 Hay, I. L. and Keller, A. *Kolloid-Z. Z. Polym.* 1965, **204**, 43
2 Hay, I. L. and Keller, A. *J. Mater. Sci.* 1966, **1**, 41
3 Keller, A. and Rider, J. G. *J. Mater. Sci.* 1966, **1**, 389
4 Hay, I. L. and Keller, A. *J. Mater. Sci.* 1967, **2**, 538
5 Cowking, A., Rider, J. G., Hay, I. L. and Keller, A. *J. Mater. Sci.* 1968, **3**, 646
6 Point, J. J., Homes, G. A., Gezovich, D. and Keller, A. *J. Mater. Sci.* 1969, **4**, 908
7 Keller, A. and Pope, D. P. *J. Mater. Sci.* 1971, **6**, 453
8 Pope, D. P. and Keller, A. *J. Mater. Sci.* 1974, **9**, 920
9 Hinton, T. and Rider, J. G. *J. Appl. Phys.* 1968, **39**, 4932
10 Rider, J. G. and Hargreaves, E. *J. Polym. Sci. (A-2)* 1969, **7**, 829
11 Young, R. J., Bowden, P. B., Ritchie, J. M. and Rider, J. G. *J. Mater. Sci.* 1973, **8**, 23
12 Meinel, G., Morosoff, N. and Peterlin, A. *J. Polym. Sci. (A-2)* 1970, **8**, 1723
13 Meinel, G. and Peterlin, A. *J. Polym. Sci. (A-2)* 1971, **9**, 67
14 Meinel, G. and Peterlin, A. *Eur. Polym. J.* 1971, **7**, 657
15 Meinel, G. and Peterlin, A. *Kolloid-Z. Z. Polym.* 1970, **242**, 1151
16 Kawai, H. and Narida, K. *Kobunshi* 1964, **13**, 585
17 Oda, T. and Kawai, H. *Kobunshi* 1969, **18**, 405
18 Brown, N. and Ward, I. M. *Phil. Mag.* 1968, **17**, 961
19 Brown, N. and Ward, I. M. *J. Polym. Sci. (A-2)* 1968, **6**, 607
20 Brown, N., Duckett, R. A. and Ward, I. M. *Phil. Mag.* 1968, **18**, 483
21 Brown, N., Duckett, R. A. and Ward, I. M. *J. Phys. D: Appl. Phys., Ser. 2* 1968, **1**, 1369
22 Richardson, I. D. and Ward, I. M. *J. Phys. D: Appl. Phys.* 1970, **3**, 643
23 Richardson, I. D., Duckett, R. A. and Ward, I. M. *J. Phys. D: Appl. Phys.* 1970, **3**, 649
24 Parrish, M. and Brown, N. *J. Macromol. Sci., Phys.* 1970, **B4**, 649
25 Duckett, R. A., Goswami, B. C. and Ward, I. M. *J. Polym. Sci., Polym. Phys. Edn* 1977, **15**, 333
26 Robertson, R. E. and Joynson, W. *J. Appl. Phys.* 1966, **37**, 3969
27 Robertson, R. E. *J. Polym. Sci. (A-2)* 1969, **7**, 1315
28 Robertson, R. E. *J. Polym. Sci. (A-2)* 1971, **9**, 1255
29 Tajima, Y. *Japanese J. Appl. Phys.* 1973, **12**, 40
30 Hibi, S., Suzuki, K., Hirano, T., Torii, T., Fujita, K., Nakanishi, E. and Maeda, M. *Kobunshi Ronbunshu* 1988, **45**, 237
31 Katagiri, T., Sugimoto, M., Nakanishi, E. and Hibi, S. *Polymer* 1993, **34**, 487
32 Wang, M.-D., Nakanishi, E. and Hibi, S. *Polymer* 1993, **34**, 2792
33 Tashiro, K., Kobayashi, M. and Tadokoro, H. *Macromolecules* 1977, **10**, 731
34 Ward, I. M. *Proc. Phys. Soc. A* 1962, **80**, 1176
35 Hill, R. *Proc. R. Soc. A* 1968, **193**, 281